Available online at www.sciencedirect.com
ScienceDirect
Trans. Nonferrous Met. Soc. China 26(2016) 2442−2448
Transactions of Nonferrous Metals Society of China
www.tnmsc.cn

Effect of gap generator blank thickness on formability in multilayer stamp forming process

Rong-jing ZHANG, Li-hui LANG, Rizwan ZAFAR, kui LI, lei WU

School of Mechanical Engineering and Automation, Beihang University, Beijing 100191, China

Received 7 September 2015; accepted 22 March 2016

Abstract: Experimental and numerical analyses for the effect of the thickness of gap generator blank (GGB) on the formability of the outer blanks were investigated. The thickness of the GGB has the greatest impact on the thinning of the lowest blank. In addition, the friction at different regions and the additional interlayer contacts can also affect the thinning of different regions as well as increase the punch force. This work will enhance the understanding of simultaneous multi-layered blanks forming and will help the composite design engineers to tailor requirement-specific hybrid parts such as fiber metal laminates (FMLs) and functionally graded structures (FGSs) for hi-tech applications.

Key words: gap generator blanks (GGB); thinning; friction; punch force; hybrid part

1 Introduction

Fiber metal laminates (FMLs) have been widely used in aerospace structures and infrastructure due to their light weight and high specific strength. There are two common techniques being used to make FMLs. The first method is used to make huge FML structures which are comparatively simple in design by autoclave, such as wings and aircraft's skins [1−3]. The second method is applied to the stamp forming (die/punch etc.) to fabricate relatively small, deep drawn, complex profiled parts using thermoplastic resins such as polypropylene-based short fiber metal laminates [4−8]. ZAFAR et al [9−12] recently proposed and demonstrated the concept of simultaneous forming method (the 3A method) for multilayer metallic blanks, which ultimately facilitates the manufacturing of tailor-made FMLs and functionally gradient structures (FGSs). In contrast with the existing methods used to make FML parts, this new approach eliminates the prerequisite of heating/solidification/reheating of the blank assembly/tooling and the requirements to strictly control the stamp forming parameters such as the punch and the binder forces. The 3A method can only be used for forming products which have a uniform gap as shown in Fig. 1(a). One of the major drawbacks of applying the "3A Method" is the absence of gap between the simultaneously formed layers when vertical features are formed such as in deep drawn cylindrical parts, as shown in Fig. 1(b). In order to solve this problem, an "improved 3A method" based on the provision of extra "gap generator" blank between the inter layers has been devised and implemented in this research. The concepts of the 3A and the improved 3A methods (GGB strategy) are reproduced in Fig. 2 for easy comprehension in this work. After simultaneous forming of the metallic blanks assembly, GGB can be separated by mechanical/thermal means and the required composite materials (weavings/unidirectional/chopped/self-reinforced polymers, etc.) can be placed at any desired areas with a freedom to use the thermosetting (TS) or thermoplastic (TP) resins. While the existing methods can only employ short/chopped fibers with TP resins because the woven fabric/long fibers can easily be ruptured using existing methods. Furthermore, the needs to make a different set of tooling (punch/die) for each layer of the multi-structural part are also eradicated. A detailed literature survey and discussion about the advantages of the simultaneous forming method (the 3A method), the limitations of the existing methods and the motivation to conduct the present study were described in Refs. [13−18].

Foundation item: Project (2010DFA52030) supported by the International Scientific Cooperation, China; Project (51175024) supported by the National Natural Science Foundation of China
Corresponding author: Rong-jing ZHANG; Tel: +86-10-82317062; E-mail: zrjbuaa@163.com
DOI: 10.1016/S1003-6326(16)64364-9

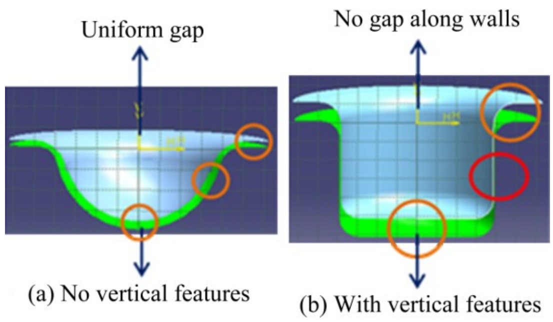

Fig. 1 Gap variations with shape change: (a) Part without any vertical feature; (b) Part having vertical features

GGB thickness is one of the most important material design parameters, which needs to be considered during the FML or FGS parts design planning stage. This gap determines the thickness/quantity/volume of the composite sheets (woven fabric/sheets/resin) or the weight/volume of the fibers (short/chopped fibers/resin) which could be placed in that space after forming and disassembly of the blank layers. After disassembling the formed metallic layers, the GGB is removed. The mechanical/thermal/chemical properties of the laminated part are ultimately designed and controlled by the gap produced by the GGB. Since, during a plastic deformation process like the deep drawing, the stresses in the flange, walls and the bottom of a cylindrical part are different and hence the strain states are also different. Especially, when multiple metallic layers are formed using the same punch and force, the forming behavior of layers with different thicknesses may not be similar. This study will investigate the effect of the different thicknesses of GGB and the forming behavior of the thinner blanks around it. In order to get a clear evaluation, most of the parameters such as material, diameter, target forming depth, punch speed, coefficients of friction and formed diameters of the multilayer parts are kept similar. However, the layup configurations and the thicknesses of the GGB are changed to draw a three-layer structure. It is important to emphasize that using the GGB strategy (the improved 3A method) to form the multilayer metallic structure as a framework to make complex hybrid parts is the latest methodology and rare literature is available in this regard.

2 Numerical simulation and experimental setup

Aluminum alloys Al2024-O having a diameter of 140 mm were used to the three-layer forming simulations. Thickness combinations and the tensile properties of the alloy are given in Table 1. The tensile test was performed according to ASTM E8 at room temperature using

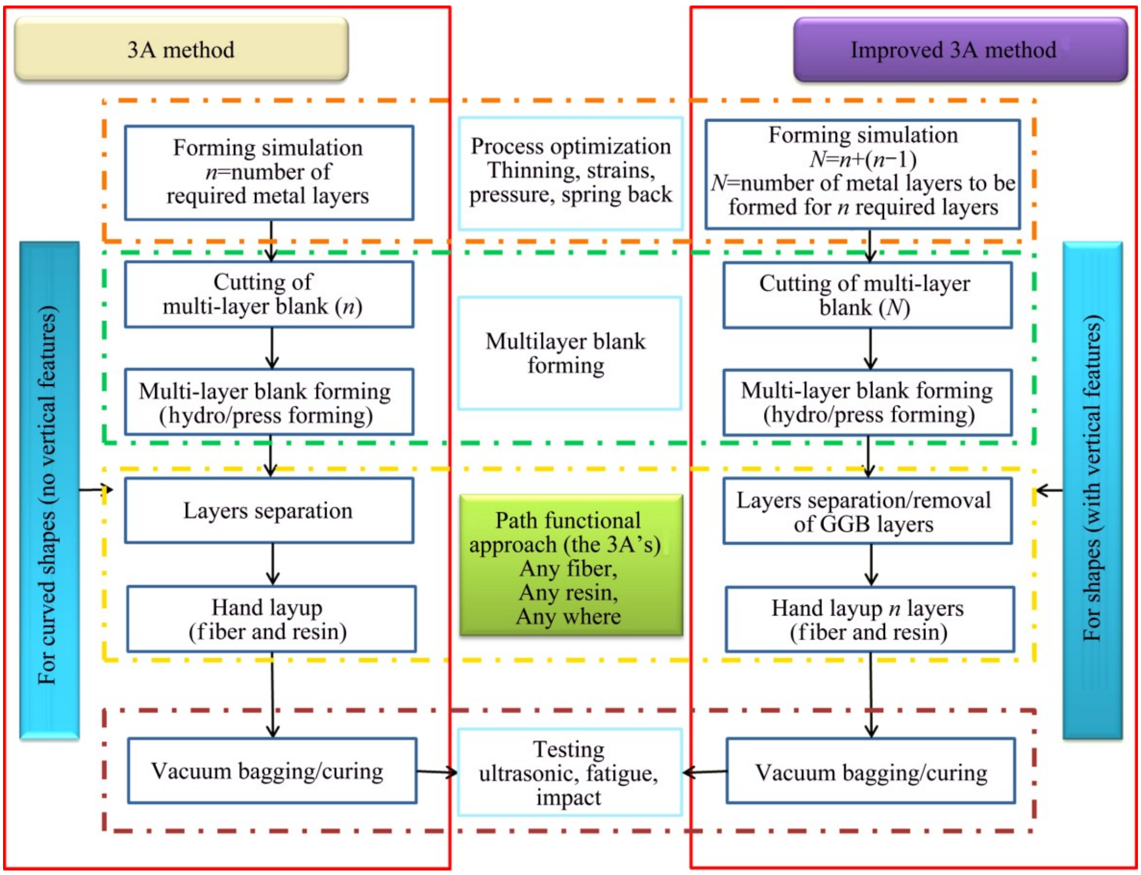

Fig. 2 3A and improved 3A methods (GGB strategy)

Table 1 Thickness combinations and tensile strength properties of Al2024-O

Sample No.	Constituent layer	Thickness/ mm	BHF/ kN	UTS/MPa	Yield strength at 0.2%/MPa	*E*/GPa	Poison ratio	*r*-values at 0°, 45°, 90°
1	0.5+0.5+0.5	1.5	20	195.33	110.55	62.25	0.33	0.85, 0.77, 2.45
2	0.5+1.0+0.5	2.0	30	198.2	113.30	63.54	0.33	0.79, 0.81, 2.40
3	0.5+1.5+0.5	2.5	40	197	112.2	64.33	0.33	0.82, 0.83, 2.1

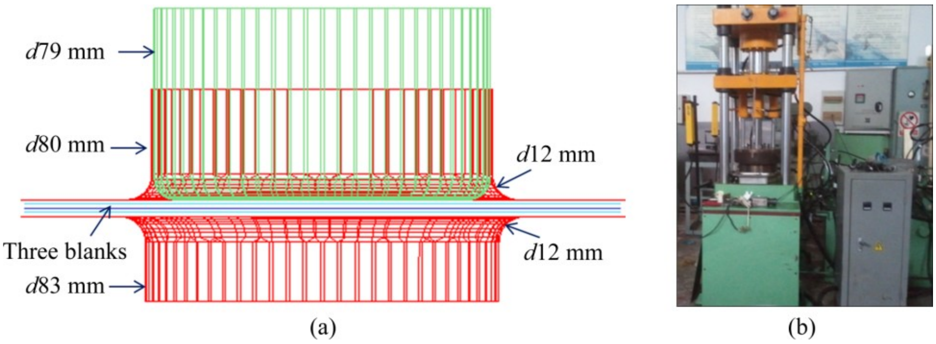

Fig. 3 Simulation setup for 3 layers of blank assembly (a) and press forming equipment (b)

rectangular, dog bone-shaped tensile test specimens which were sliced along the rolling direction (RD) and Instron 5900 testing machine was used. The length and width of tensile test samples were 210 and 20 mm, respectively. Different thicknesses of Al2024-O were achieved by combining 0.5 mm-thick tensile test samples to see the cumulative effect of multilayered forming on tensile properties as shown in Table 1. Thickness of the formed sample layers was measured by using the ultrasonic thickness tester.

36*MAT_3PARAMETER_BARLAT code of DYNAFORM/LS Dyna was used to simulate the forming behavior of three-layered blanks by considering the high anisotropic characteristics of the alloy. Figure 3(a) illustrates the numerical simulation setup devised for the simultaneous forming of three layers. Stress−strain curve was imported into the material mode of the software, which automatically calculates the values of strain hardening index n and material hardness coefficient K. All the tools including punch, die and blank holder were treated as rigid bodies with mesh size of 30 mm. Blanks were treated as deformable bodies with mesh size of 3 mm and quadrangle shape elements. Coefficients of friction for the die, punch and binder were assumed to be 0.05, 0.15 and 0.1, respectively. Surface to surface and one way surface to surface contact modes available in the DYNAFORM were used to model the contacts between blanks and the contacts between the blanks and tooling, in that order. Numerous simulations were run to find the most suitable values of BHF at the no die-binder gap conditions to carry out the experiments.

Hydroforming machine as shown in Fig. 3(b) was used (without employing the HF function) to study the deep drawing behavior of the multilayer blanks. The machine is controlled through a hydraulic feed controller, the dynamics of which is provided by a hydraulic oil filled accumulator and is charged by using a two-stage pump located next to the machine. All test conditions including blank holder force, feed rate and post-forming holding time could be set up through the software installed in the computer that is embedded in the machine. Cylindrical shaped punch having 79 mm diameter was used to form the blanks up to the target depths.

3 Results and discussion

3.1 Effect of GGB thickness on thinning of blanks

Figure 4 describes the measured and numerical values of thinning of the three blanks assemblies drawn at different BHF values up to 30 mm in depth, which are in reasonable agreement with each other. Red and black encircled regions in Fig. 4 show the highest and the second highest thinning regions during simultaneous, multilayered forming of the three-layer alloy for different thicknesses of the GGB (Blank2), respectively. These two regions include the vertical wall area of the formed part below the die bending radius (region-1) and the punch corner radius area (region-2). From Fig. 4, it can be found that the lowermost blank, i.e., the Blank1 suffers the maximum thinning among the three blanks formed together. Furthermore, it is worthwhile to note that the thickness of the GGB has an important impact on the thinning of the whole structure as it controls the thinning of its outer layers. Also, the values of the thinning decrease from the lower layers to the upper layers at the two critical regions. For a GGB thickness of

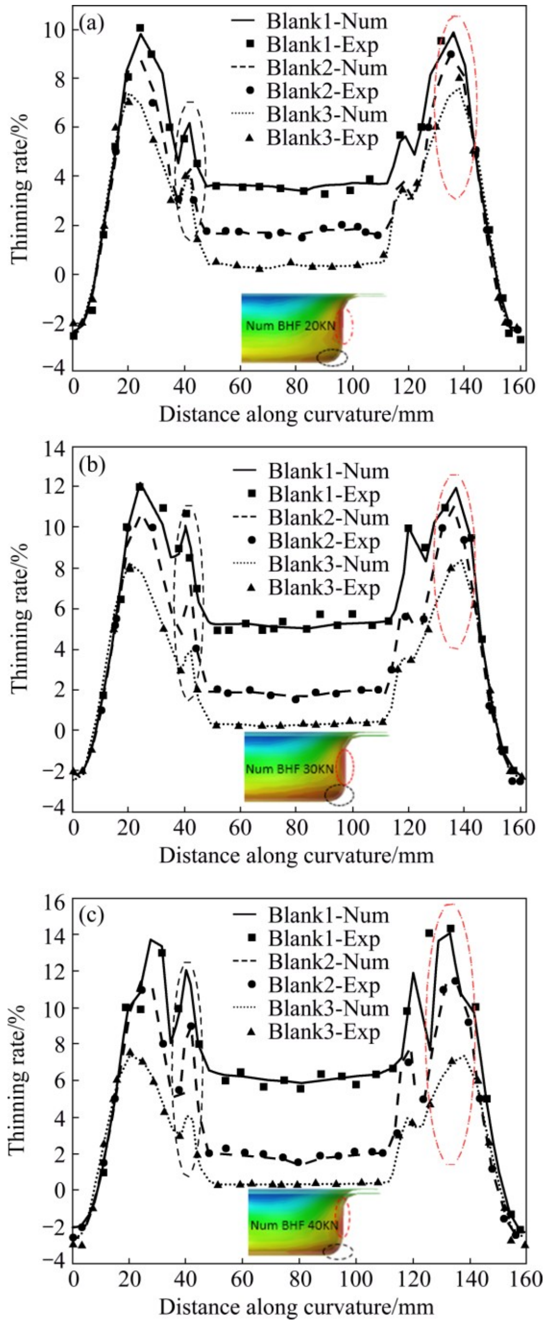

Fig. 4 Experimental and numerical values of thinning of three blanks assemblies drawn at different thicknesses of GGB: (a) 0.5 mm; (b) 1.0 mm; (c) 1.5 mm

0.5 mm, region-1 undergoes a maximum thinning (9.8%) while the region-2 withstands a maximum thinning (5.9%) for the Blank1. The same trend of the thickness variation can be noticed for the Blank1 of the assemblies with GGB thicknesses of 1.0 and 1.5 mm having maximum thinning values of 12% and 13.8% for the region-1 and 10% and 12% for the region-2. Also, the height of the second region peaks keeps on increasing with the increase in the thickness of GGB while the thinning for the Blank3 almost remains unchanged at all the regions for different GGB thicknesses. The relative thinning of the three middle blanks (Blank2) of the three different blank assemblies is also shown in Fig. 5 to clarify the effect of GGBs thickness on their thinning rate.

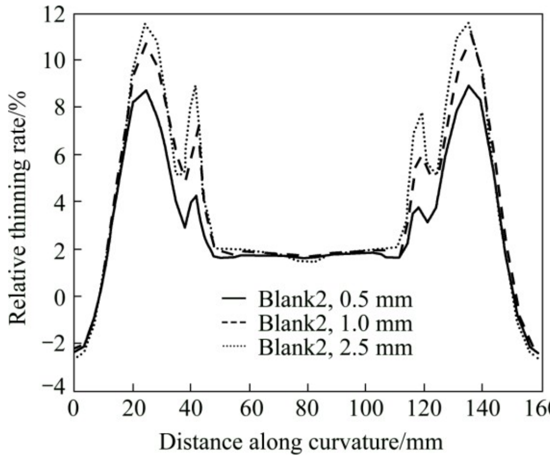

Fig. 5 Thinning of Blank2 with various thicknesses in three assemblies

These observations can be explained in the light of relative movement between the constituent layers of a blank assembly due to different frictional forces and the varying distances of layers from the punch as shown in Fig. 6(a). The relative movement is because of higher

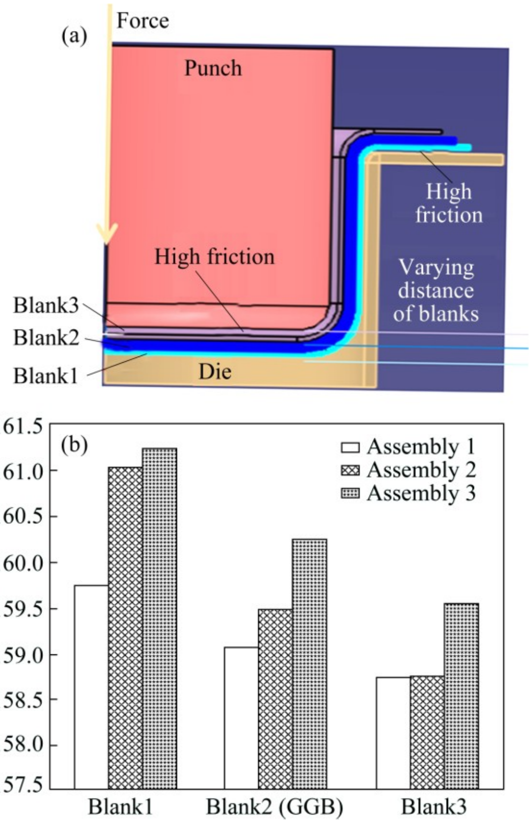

Fig. 6 Thinning of Blank2 with various thicknesses in three assemblies (a) and curvature lengths in various blank assemblies (b)

friction which acts at the Blank3/punch and Blank1/die interfaces than that of the Blank1/Blank2/Blank3 interfaces. These factors lead to different plastic deformation/metal flow rates in the three layers resulting in different arc lengths of the three blanks in a blank assembly. As the thickness of the GGB in a blank assembly is increased, the distance of Blank1 from the punch is also increased with an increased arc length, which results in more thinning of the blanks in critical regions such as the punch radius area as illustrated in Fig. 6(b).

The three simultaneously formed blanks assemblies with varying GGB thicknesses at different BHF values are shown in Fig. 7. Experimental and numerical values of the BHF are in accord with each other and exhibit an increasing trend with the increase of the overall thickness of a blank assembly. After forming, the GGB can be separated by mechanical means and the gap generated by this blank can be utilized to place any kind of composite/resin materials according to the specific requirements by following the procedure described in Fig. 2.

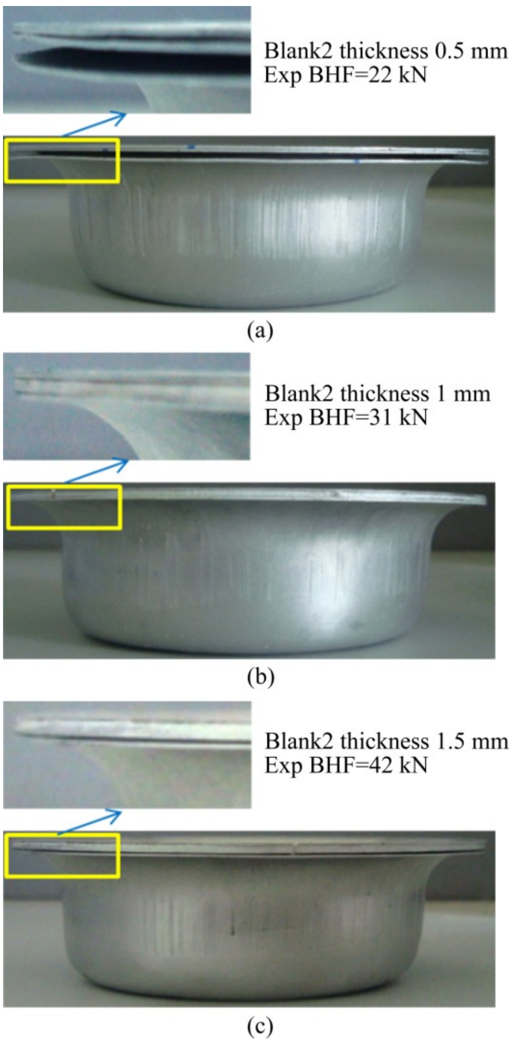

Fig. 7 Three blank assemblies formed up to 30 mm in depth with inset showing GGB

3.2 Effect of GGB thickness on punch force

Figure 8 illustrates the punch force versus displacement curves for the three types of blank assemblies. It can be seen that punch force greatly depends upon the total thickness of the blanks to be drawn and the punch force increases with the increasing of thickness. Another important point to be considered in the simultaneous and multilayer forming is the inter-layer friction which is not present in monolithic deep drawing. These additional inter-layer contacts also play a role in increasing the force needed to deform the structure and cause fluctuations/variations in force which can be seen from the curves. However, further investigation is needed to explore the mechanics theory and the role of friction.

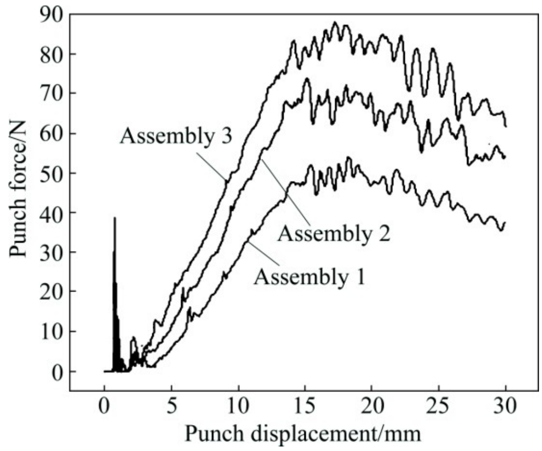

Fig. 8 Punch force versus displacement curve for three blank assemblies

3.3 Effect of GGB thickness on increased forming depths

The experimental study was further extended to determine the role of the GGB at increased forming depths and the failure mechanism as well. To this end, more sets of blank assembly types 1 and 3 were used and the experiment was repeated twice to validate the results under the same experimental conditions as being used to form 30 mm-deep samples. Figure 9 demonstrates the parts made by using this phase of study. As can be seen in Fig. 9(a), the forming depth for blank assembly 1 having 0.5 mm-thick GGB is 40 mm. At this depth, a fracture can be observed at punch radius area of the Blank1 only when the other blanks are safe. For blank assembly 3, which contains a 1.5 mm-thick GGB, the forming depth is 33 mm at which fracture occurs, as shown in Fig. 9(b). Due to the presence of a thicker GGB (such as 1.5 mm in thickness) in the middle, the arc formed at the punch radius area for Blank1 (blank assembly 3) is much larger compared with both the other two blanks of this assembly and the Blank1 of blank assembly 1. Due to a larger arc, a higher tensile stress state exists at punch radius area together with the stress concentration factor due to shape change. This high tensile stress state results in necking of the material at this area, which ultimately leads to fracture.

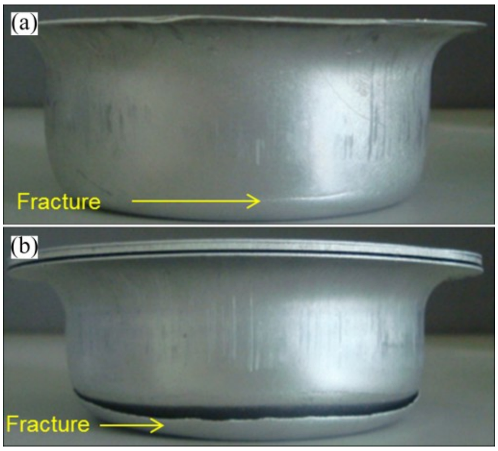

Fig. 9 Comparsion of forming depths for blank assembly 1 (a) and blank assembly 3 (b)

From the above discussion, we can learn that using the GGB during simultaneous forming is a novel and practicable concept and it is potentially possible to replace the existing stamp forming methods which are used to fabricate FMLs as described in the literature. The currently available techniques can only form simple shapes such as hemispherical parts. If the GGB method can be applied, complex shapes with sharp bends such as the cylindrical parts manufactured in this study can also be efficiently formed. The repeated heat and re-solidification steps can be eliminated with a freedom to place any kind of resins (TP/TS) and composites at any required place. The research can be applied to replacing the monolithic metallic parts used in the aerospace and automobiles industries with the hybrid parts such as covers, casings, housings, panels and other shapes.

4 Conclusions

1) The thickness of the GGB has the greatest impact on the thinning of the lowermost blank due to its maximum distance from the punch and the resulting larger curvature length. Therefore, the thickness of the GGB and the outer layers must be carefully selected keeping in view the forming depth.

2) Different frictions at different regions of the formed part and the presence of additional inter-layer contacts also play critical roles for varying thinning at different regions as well as increasing the punch force.

3) The research will help in understanding the physical phenomenon occurring during simultaneous forming of multilayer blanks and will increase the application areas of the new methodology.

References

[1] PARK S Y, CHOI W J, CHOI H S. A comparative study on the properties of GLARE laminates cured by autoclave and autoclave consolidation followed by oven postcuring [J]. Int J Adv Manuf Tech, 2010, 49: 605−613.

[2] KUMAR K V, SAFIULLAH M, AHMAD A N K. Root cause analysis of heating rate deviations in autoclave curing of CFRP structures [J]. Int J Innov Res Stud, 2013, 2(5): 369−378.

[3] BOTELHO E C, SILVA R A, PARDINI L C, REZENDE M C. A review on the development and properties of continuous fiber/epoxy/ aluminum hybrid composites for aircraft structures [J]. Materials Research, 2006, 9(3): 247−256.

[4] SINMAZCELIK T, AVCU E, BORA M Ö, ÇOBAN O. A review: Fibre metal laminates, background, bonding types and applied test methods [J]. Materials & Design, 2011, 32(7): 3671−3685.

[5] MOSSE L, COMPSTON P, CANTWELL W J, CARDEW-HALL M, KALYANASUNDARAM S. The effect of process temperature on the formability of polypropylene based fibre–metal laminates [J]. Composites Part A: Applied Science and Manufacturing, 2005, 36(8): 1158−1166.

[6] TAKAMATSU T, MATSUMURA T, OGURA N, SHIMOKAWA T, KAKUTA Y. Fatigue crack growth properties of a GLARE3-5/4 fiber/metal laminate [J]. Engineering Fracture Mechanics, 1999, 63(3): 253−272.

[7] KALYANASUNDARAM S, DHARMALINGAM S, VENKATESAN S, SEXTON A. Effect of process parameters during forming of self reinforced–PP based fiber metal laminate [J]. Composite Structures, 2013, 97: 332−337.

[8] BOISSE P, HAMILA N, VIDAL-SALLÉ E, DUMONT F. Simulation of wrinkling during textile composite reinforcement forming: Influence of tensile, in-plane shear and bending stiffnesses [J]. Composites Science and Technology, 2011, 71(5): 683−692.

[9] ZAFAR R, LANG L, ZHANG R. Experimental and numerical evaluation of multilayer sheet forming process parameters for light weight structures using innovative methodology [J]. International Journal of Material Forming, 2016, 9(1): 35−47.

[10] ZHANG R, LANG L, ZAFAR R, LIN L, ZHANG W. Investigation into thinning and spring back of multilayer metal forming using hydro-mechanical deep drawing (HMDD) for lightweight parts [J]. The International Journal of Advanced Manufacturing Technology, 2016, 82(5−8): 817−826.

[11] ZAFAR R, LANG L, ZHANG R. Analysis of hydro-mechanical deep drawing and the effects of cavity pressure on quality of simultaneously formed three-layer Al alloy parts [J]. The International Journal of Advanced Manufacturing Technology, 2015, 80(9−12): 2117−2128.

[12] ZHANG R, LANG L, ZAFAR R. FEM-based strain analysis study for multilayer sheet forming process [J]. Frontiers of Mechanical Engineering, 2015, 10(4): 373−379.

[13] GRESHAM J, CANTWELL W, CARDEW-HALL M J, COMPSTON P, KALYANASUNDARAM S. Drawing behaviour of metal–composite sandwich structures [J]. Composite Structures, 2006, 75(1): 305−312.

[14] HOU M. Stamp forming of continuous glass fibre reinforced polypropylene [J]. Composites Part A: Applied Science and Manufacturing, 1997, 28(8): 695−702.

[15] YANG Xi-ying, LANG Li-hui, LIU Kang-ning, GUO Chan. Modified MK model combined with ductile fracture criterion and its application in warm hydroforming [J]. Transactions of Nonferrous Metals Society of China, 2015, 25(10): 3389−3398.

[16] HWANG S F, HWANG K J. Stamp forming of locally heated thermoplastic composites [J]. Composites Part A: Applied Science and Manufacturing, 2002, 33(5): 669−676.

[17] RAJABI A, KADKHODAYAN M, MANOOCHWHRI M, FARJADFAR R. Deep-drawing of thermoplastic metal-composite structures: Experimental investigations, statistical analyses and finite element modeling [J]. Journal of Materials Processing Technology, 2015, 215: 159−170.

[18] JALIL A, GOLLO M H, SHEIKHI M M, SEYEDKASHI S H. Hydrodynamic deep drawing of double layered conical cups [J]. Transactions of Nonferrous Metals Society of China, 2016, 26(1): 237−247.

间隙产生层板的厚度对多层板拉深成形的影响

张容静，郎利辉，Zafar RIZWAN，李 奎，吴 磊

北京航空航天大学 机械工程及自动化学院，北京 100191

摘　要：通过数值模拟与试验研究间隙产生层板的厚度对多层板中最外层板的成形性能的影响。研究结果表明，间隙产生层板的厚度对最底层板减薄的影响最大。此外，不同部位的摩擦和中间层板间的接触对不同位置的减薄也有影响，并且凸模力随着摩擦力的增加而增大。通过该研究可以加深对多层板同步成形的认识，并且能帮助复合材料工程师设计生产出如纤维增强金属层板和功能梯度构件等具有特殊要求的高性能混合零件。

关键词：间隙产生层板；减薄；摩擦；凸模力；混合零件

(Edited by Xiang-qun LI)